Homoleptic Rare-Earth Carbazolates and the Trends of Their $E_{Ln^{II/III}}$ Redox Potentials: Mixed-Valent Samarium in $^1_\infty[Sm_2(Cbz)_5](CbzH)$ (CbzH = carbazole) and Trivalent Thulium, Neodymium and Gadolinium in $[Ln_2(Cbz)_6]$

Klaus Müller-Buschbaum*[a] and Catharina C. Quitmann[a]

Keywords: Solvent-free synthesis / Lanthanides / Carbazolates / N ligands

The solvent-free melt reaction of carbazole (CbzH, $C_{12}H_8NH$) with samarium metal yields $^1_\infty[Sm_2(Cbz)_5](CbzH)$ (**1**), whilst the melt reactions with thulium, neodymium and gadolinium give $[Tm_2(Cbz)_6]$ (**2**), $[Nd_2(Cbz)_6]$ (**3**) and $[Gd_2(Cbz)_6]$ (**4**), respectively. Compounds **1** and **2** were obtained as single crystals and their crystal structures determined by single-crystal X-ray analysis, whilst **3** and **4** were obtained as powders. X-ray powder diffraction studies show that the gadolinium-containing complex **4** is isotypic to the thulium complex **2**, whereas the neodymium-containing complex **3** is not. Compound **1** contains alternating Sm^{II} and Sm^{III} cations in a chain structure. Complex **2** only exhibits dimeric units of Tm^{III}. Besides Ln–N coordination, the crystal structures of both compounds show η^6-π interactions with the phenyl rings of the carbazolate ligands. This leads to small coordination polyhedra, such as connected tetrahedra of two nitrogen atoms and two η^6-π-coordinated phenyl rings around Sm^{II}, and trigonal bipyramids of five nitrogen atoms around Sm^{III} for **1**, as well as tetrahedra of three nitrogen atoms and one η^6-π-phenyl interaction around Tm^{III} for **2**. From the trend of the $E_{Ln^{II/III}}$ redox potentials, the complexes of neodymium and gadolinium are also trivalent. For **1**–**4** the results of FIR, MIR and Raman spectroscopy as well as simultaneous DTA/TG analyses are also presented.

Introduction

Since the syntheses of the first cyclopentadienyl complexes[1] and metallocenes[2] solvent-containing reaction routes have come to dominate all fields of rare-earth-metal coordination chemistry.[3−7] Accordingly, the vast majority of structurally characterised compounds are solvates and are therefore heteroleptic[8] whenever the ligands do not meet certain criteria like multi-chelating, such as in the rare-earth-metal amide complexes.[8−11] The reactivity of rare-earth metals themselves has proven to be high enough to be able to react directly with amines, yielding homoleptic amides. Whilst initial work with substituted pyrazolate ligands made solvent recrystallisation[12,13] steps necessary in order to obtain crystalline products, we have systematically developed a type of solvent-free melt synthesis that allows the crystallisation of products under reaction conditions,[14−17] including the first homoleptic carbazolates of europium and ytterbium;[18] heteroleptic solvent-containing carbazolates have been reported previously.[19,20] Both europium and ytterbium carbazolates are divalent. Therefore, reactions of samarium, thulium, neodymium and gadolinium metal with carbazole were carried out, their reaction products $^1_\infty[Sm_2(Cbz)_5](CbzH)$ (**1**) and $[Ln_2(Cbz)_6]$ [Ln = Tm, Nd, Gd (**2**−**4**)] illuminating the trend of the $E_{Ln^{II/III}}$ redox potentials[21,22] (see Scheme 1) from Eu^{II} and Yb^{II} in $^1_\infty[Ln_2(Cbz)_4]$[18] to mixed-valent Sm^{II}/Sm^{III} and trivalent Tm^{III}, Nd^{III} and Gd^{III}. The results are compounds with different crystal structures that are unique in rare-earth-metal amide chemistry.

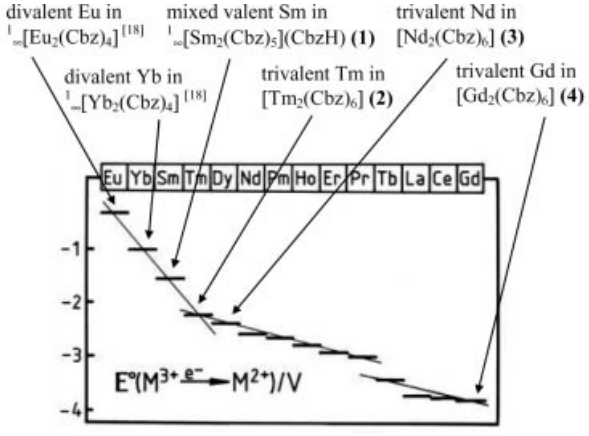

Scheme 1. Homoleptic rare-earth carbazolates and their $E_{Ln^{II/III}}$ redox potentials[21,22] (diagram taken from ref.[22] with permission of the author)

Results and Discussion

The solvent-free reactions of samarium, thulium, neodymium and gadolinium with carbazole were carried out in

[a] Institut für Anorganische Chemie, Universität zu Köln, Greinstrasse 6, 50939 Köln, Germany
E-mail: Klaus.Mueller-Buschbaum@Uni-Koeln.de

  DOI: 10.1002/ejic.200400516

a melt of the amine in ampoules. The reaction with samarium metal yielded black, in thin layers dark red crystals of $^1_\infty[Sm_2(Cbz)_5](CbzH)$ (**1**) at 270 °C [Equation (1)]. Activation by amalgamation dropped the reaction temperature to 255 °C but decreased the crystallinity of the bulk product. No further reaction to the trivalent state was observed up to decomposition (see Figure 1), even when an excess of CbzH was used.

$$Ln + x\,HN(R_2) \rightarrow Ln(NR_2)_x + x/2\,H_2 \quad (1)$$

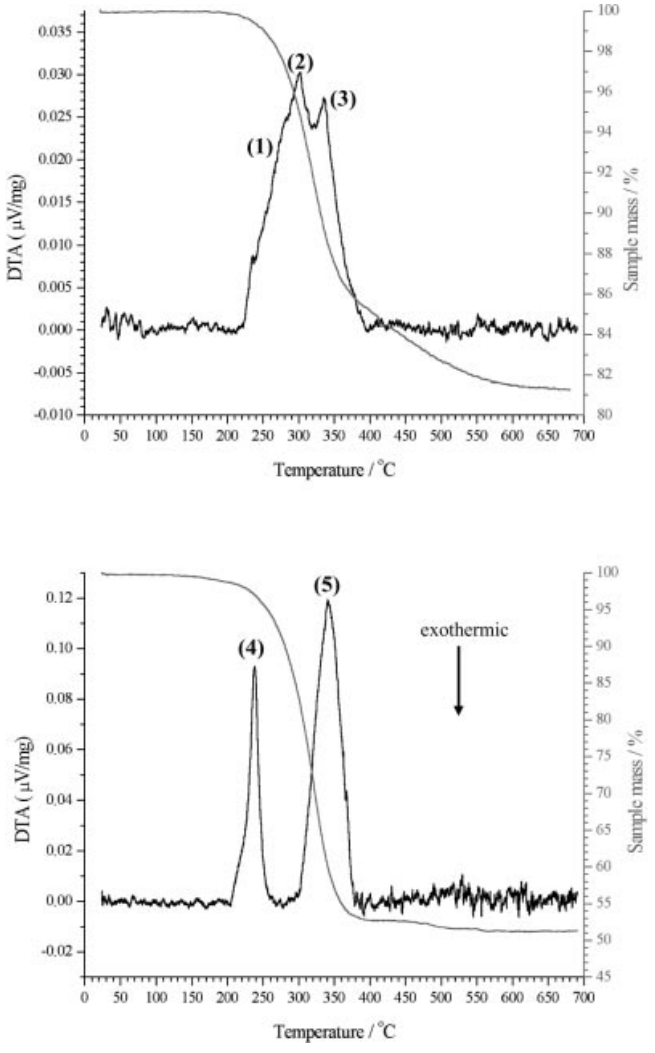

Figure 1. The thermal decompositions of $^1_\infty[Sm_2(Cbz)_5](CbzH)$ (**1**, top) and $[Tm_2(Cbz)_6]$ (**2**, bottom) investigated by simultaneous DTA/TG in the temperature range 20−700 °C; the plot of the bulk material of **1** exhibits the melting point of excess carbazole (1), release of uncoordinated carbazole from the structure (2) and the decomposition (3) of **1**; the thermal investigation of the bulk material of **2** exhibits the melting point (4) and the decomposition (5) of **2**; neither excess nor uncoordinated carbazole is observed for **2**

The reaction with thulium metal was also carried out under solvent-free conditions in a carbazole melt except that both amalgam activation of Tm and a reaction temperature of 280 °C were necessary to obtain orange to red crystals of $[Tm_2(Cbz)_6]$ (**2**).

Neodymium and gadolinium metal react with carbazole only as an amalgam containing at least one tenth of the amount of the rare-earth metal. A reaction temperature of 280 °C was also necessary to obtain $[Nd_2(Cbz)_6]$ (**3**) as a golden-yellow solid. $[Gd_2(Cbz)_6]$ (**4**) was formed upon annealing at 245 °C already, following activation at 280−290 °C, giving a poorly crystalline dark yellow solid.

The thermal decomposition of **1**−**4** was investigated by simultaneous DTA/TG.[23] This method has already proved its value for understanding comparable melt reactions with 2-(2-pyridyl)benzimidazole[15] and shows the decomposition path of the bulk product of the melt reaction. This analysis provides additional information regarding the completeness of the reaction and possible phase impurities.

$^1_\infty[Sm_2(Cbz)_5](CbzH)$ (**1**) is a molecular polymer formed at relatively high temperatures (255−270 °C). Accordingly, its thermal behaviour and stability must be different from the known heteroleptic carbazolates, and therefore the bulk product of the synthesis was studied. Although the thermogravimetric investigation displays no separated signals, the resolution of the differential thermoanalysis exhibits three different signals (Figure 1, top). The first signal in the heat flow was identified as the melting point of unchanged carbazole at 235 °C, followed by a slight mass loss of the excess carbazole (about 2%) displayed by a shoulder of an endothermic peak in the heat flow. At a reaction temperature of 270 °C, $^1_\infty[Sm_2(Cbz)_5](CbzH)$ slowly starts to decompose without melting and releases the uncoordinated CbzH (M = 167.1 g/mol; calcd. 12.9% of $M\{^1_\infty[Sm_2(Cbz)_5](CbzH)\}$; found 13%). At 290−300 °C another endothermic signal is observed that indicates further thermal decomposition of $^1_\infty[Sm_2(Cbz)_5]$ without the formation of defined decomposition products. The unseparated thermal signals indicate that the later processes begin before the earlier ones are completely finished. Although the thermal stability of $^1_\infty[Sm_2(Cbz)_5](CbzH)$ is high, it does not reach the stability of the homoleptic divalent rare-earth carbazolates.[18] One of the reasons for this behaviour could be the unsaturated coordination spheres of the samarium atoms. Considering the formation temperature of 270°C, the temperature frame to obtain the compound is very limited and it is neither likely that $^1_\infty[Sm_2(Cbz)_5]$ is obtained free of CbzH by the melt synthesis nor that $^1_\infty[Sm_2(Cbz)_5](CbzH)$ forms if the volatile CbzH is not forced to stay in the reaction mixture, as provided by the ampoule treatment.

The thermal decompositions of $[Ln_2(Cbz)_6]$ [Ln = Tm, Nd, Gd (**2**−**4**)] are relatively similar to each other, but different from **1** due to their different structures. All three compounds show sharp melting points of the products as well as one following endothermic decomposition step. Complexes **2**−**4** have much lower melting points (220 °C for **2**, 190 °C for **3** and 175 °C for **4**; see Figure 1 for Tm) than the polymeric carbazolates $^1_\infty[Ln_2(Cbz)_4]$ (Ln = Eu, Yb).[18] The melting points are identified by sharp endothermic peaks in the heat flow with no related mass loss.

The subsequent decomposition step for **2** starts at 300 °C with release of 47% of the sample mass. For **3** the decomposition starts at 310 °C with release of 68% of the sample mass. This includes 15% of unchanged carbazole in the bulk sample, as identified by its melting point, and an additional endothermic signal in the heat flow. The behaviour of **4** is similar, its decomposition starting at 270 °C with 3% of unchanged carbazole being released prior to a mass loss of 51%. In contrast to **1**, **3** and **4** the bulk sample of **2** is free of unchanged carbazole, indicating complete reaction. Although the volatile products of the decompositions of **2**−**4** could not be defined, the decomposition pathways are likely to be similar for all three compounds because the released sample masses match the different molecular masses of Tm, Gd and Nd. The decomposition temperatures of **1**−**4** are distinctively lower than for the divalent compounds $^1_\infty[Ln_2(Cbz)_4]$ (Ln = Eu, Yb).[18] As for the rare-earth pyridylbenzimidazolates,[15] no periodic behaviour through the course of the rare earth elements is observable either for melting points or absolute thermal stability of rare earth carbazolates, although the influence of structural characteristics is clearly evident.

The FIR and Raman spectra of **1**−**4** show bands that cannot be identified with the ligand and thus represent the Ln−N stretching modes {$^1_\infty[Sm_2(Cbz)_5](CbzH)$ (**1**): FIR: $\tilde{\nu}$ = 231, 171, 123, 108 cm^{-1}; $[Tm_2(Cbz)_6]$ (**2**): FIR: $\tilde{\nu}$ = 251, 188, 158 cm^{-1}; Raman: $\tilde{\nu}$ = 251, 200, 170 cm^{-1}; $[Nd_2(Cbz)_6]$ (**3**): FIR: $\tilde{\nu}$ = 221, 145, 123 cm^{-1}; Raman: $\tilde{\nu}$ = 280, 230 cm^{-1}; $[Gd_2(Cbz)_6]$ (**4**): FIR: $\tilde{\nu}$ = 243, 231, 159 cm^{-1}; Raman: $\tilde{\nu}$ = 297, 258, 240 cm^{-1}}. The bands thereby match well with other Ln−N-containing compounds such as rare-earth porphyrin complexes,[24] dipyridylamides[16] or pyridylbenzimidazolates[14,15] regarding the coordination spheres, valences and ionic radii in **1** to **4**. They are also in good accordance with the homoleptic carbazolates of divalent Eu and Yb.[18] The ligand lattice stretching modes are reflected by rather broad bands (FIR: $\tilde{\nu}$ = 419, 145 cm^{-1}). The MIR and Raman spectra also contain vibrational bands of the carbazolate ligands that are independent of the rare-earth ion and can therefore be assigned to CbzH[18] (**1**: IR: $\tilde{\nu}$ = 3049, 1603, 1493, 1450, 1326, 1288, 1236, 1106, 750, 725, 574 cm^{-1}; **2**: IR: $\tilde{\nu}$ = 3050, 1602, 1493, 1450, 1327, 1287, 1239, 1108, 749, 726, 574 cm^{-1}; Raman: $\tilde{\nu}$ = 1483, 1450, 1316, 1015, 744 cm^{-1}; **3**: IR: $\tilde{\nu}$ = 3049, 1601, 1493, 1450, 1327, 1287, 1238, 1107, 748, 725, 574 cm^{-1}; Raman: $\tilde{\nu}$ = 1480, 1311, 1011, 741 cm^{-1}; **4**: IR: $\tilde{\nu}$ = 3050, 1603, 1492, 1450, 1327, 1237, 750, 726 cm^{-1}; Raman: $\tilde{\nu}$ = 1481, 1451, 1311, 1011, 742 cm^{-1}). The region between 1100 and 1400 cm^{-1} is well known to contain the bands of extended aromatic systems.[25] Other bands are shifted by about ten wavenumbers compared to the free ligand or show band splitting due to coordination to the metal centers (**1**: IR: $\tilde{\nu}$ = 1482, 1459, 1433, 1146, 912, 569, 430 cm^{-1}; **2**: IR: $\tilde{\nu}$ = 1481, 1458, 1430, 1148, 905, 749, 432 cm^{-1}; Raman: $\tilde{\nu}$ = 1620, 1570, 1248, 540, 310 cm^{-1}; **3**: IR: $\tilde{\nu}$ = 1456, 1426, 1139, 914, 564, 425 cm^{-1}; Raman: $\tilde{\nu}$ =

Table 1. Selected distances [pm] and angles [°] for $^1_\infty[Sm_2(Cbz)_5](Cbz-H)$ (**1**) and $[Tm_2(Cbz)_6]$ (**2**); estimated standard deviations are given in parentheses

$^1_\infty[Sm_2(Cbz)_5](Cbz-H)$ (**1**)			
Sm1−C[range C(25−30)[a]]	294(2)−338(2)	Sm1−N1	281.7(9)
Sm1−C[range C(43−47)[a]]	294(2)−320(2)	Sm2−N5	236(2)
Sm1−C[average C(25−30)[a]]	314(2)	Sm2−N3	239(1)
Sm1−C[average C(43−47)[a]]	308(2)	Sm2−N1	240.2(9)
Sm1−C12	300(2)	Sm2−N4	247(1)
Sm1−C24	294(2)	Sm2−N2	248.8(9)
Sm1−cent1[b]	275(2)	Sm1−Sm2	419.3(2)
Sm1−cent2[b]	274(2)	Sm1−Sm2[a]	577.6(2)
Sm1−N2	271.8(9)	N−C(range)	137(2)−143(2)
cent1−Sm1−cent2[b]	105	N1−Sm2−N3	114.0(4)
cent1−Sm1−N2[b]	105(1)	N1−Sm2−N4	105.9(4)
cent1−Sm1−N1[b]	142(1)	N2−Sm2−N3	99.2(4)
N1−Sm1−N2	67.7(3)	N2−Sm2−N5	128.7(8)
cent2−Sm1−N1[b]	102(1)	N2−Sm2−N4	175.4(4)
cent2−Sm1−N2[b]	138(1)	N3−Sm2−N4	81.6(4)
		N4−Sm2−N5	85.9(9)
$[Tm_2(Cbz)_6]$ (**2**)			
Tm−C[range C(31−36)]	274.9(4)−288.7(3)	Tm−N2	222.4(3)
Tm−C[average C(31−36)]	282.0(4)	Tm−N3	228.2(3)
Tm−cent3[b]	244.2(4)	Tm−Tm[c]	503.9(1)
Tm−N1	220.8(3)	N−C(range)	137.4(4)−141.1(5)
cent3−Tm−N3[b]	104.8(1)	N1−Tm−N2	108.1(1)
cent3−Tm−N2[b]	112.2(1)	N1−Tm−N3	90.0(1)
cent3−Tm−N1[b]	122.8(1)	N2−Tm−N3	117.4(1)

[a] $x, -y + 3/2, z - 1/2$. [b] cent1 = centroid of the phenyl rings with the C atoms C25 to C30; cent2 = centroid of the phenyl rings with the C atoms C43 to C47; cent3 = centroid of the phenyl rings with the C atoms C31 to C36. [c] $-x, y, -z + 3/2$.

1625, 1573, 1260 cm^{-1}; **4**: IR: $\tilde{\nu}$ = 1471, 1448, 1430, 1426, 906, 750, 427 cm^{-1}; Raman: $\tilde{\nu}$ = 1624, 1570, 1261 cm^{-1}). A sharp ν(N−H) vibrational band[26] of CbzH in **1** can be observed at 3418 cm^{-1} and was confirmed by the MIR spectrum of the free ligand.[18] This band is only weak in the spectra of $[Ln_2(Cbz)_6]$ [Ln = Tm, Nd, Gd (**2**−**4**)], and here is due to excess carbazole only.

Although the formula of **1** differs by only one hydrogen atom from a formally trivalent compound like compounds **2**−**4**, the crystal structures of **1** and **2** are completely different from each other as well as from the carbazolates of divalent europium and ytterbium. Whilst the heteroleptic complexes $[Sm(Cbz)_2(THF)_4]$, $[Sm(Cbz)_2(N\text{-MeIm})_4]$[19] (N-MeIm = *N*-methylimidazole) and $[Eu(Cbz)_2(THF)_4]$[20] have monomeric structures due to solvent molecules saturating the coordination spheres, the homoleptic[27] rare-earth carbazolates exhibit larger building units in the crystal structures. Like the divalent compounds $^1_\infty[Ln_2(Cbz)_4]$ (Ln = Eu, Yb)[18] the crystal structure of $^1_\infty[Sm_2(Cbz)_5](CbzH)$ (**1**) consists of polymeric chains built of dimeric units with alternating Sm^{II} and Sm^{III} cations. Because of the mixed-valent character of **1** each dimeric unit contains 50% divalent and 50% trivalent samarium. The coordination spheres of Sm^{II} and Sm^{III} are very different so that the different valences can be clearly distinguished. The Sm^{II} atoms are surrounded by two nitrogen atoms and two η^6-coordinated π-systems resulting in a flattened tetrahedron. Distortion of the coordination polyhedron in $^1_\infty[Sm_2(Cbz)_5](CbzH)$ (**1**) can be seen in the deviations from the ideal value of 109.5° [centroid(1)−Sm^{II}−centroid(2): 105(1)°; N1−Sm^{II}−centroid(2): 102(1)°; N2−Sm^{II}−centroid(1): 105(1)°; N1−Sm^{II}−N2: 67.7(3)°]. The Sm^{II}−N distances are 271.8(9) and 281.7(9) pm, the differences being a result of asymmetric μ_2-bridging nitrogen atoms that link Sm^{II} to adjacent Sm^{III} atoms in the dimeric units. Such asymmetric bridges can also be found in $^1_\infty[Eu_2(Cbz)_4]$[18] or $[Yb_2(Cbz)_4(Phpip)_4](Phpip)_2$ (Phpip = phenylpiperazine).[28] The μ_2-coordination mode in **1** also explains the differences in Sm−N distances compared to $[Sm(Cbz)_2(THF)_4]$ and $[Sm(Cbz)_2(N\text{-MeIm})_4]$[19] with an average of 258 and 267 pm, respectively, or $\{[(CH_2)_5C(C_4H_3N)_2]Sm\}_4(THF)_2(N_2)[Na(THF)]_2{\cdot}2THF$ with 271−273 pm.[29] The distances from the Sm atoms to the π-systems of **1** are 274 pm on average (see Table 1 for detailed atom distances and bond angles of **1** and **2**). Although rarely observed, such η^6-phenyl π-interactions are known for the divalent homoleptic carbazolates[18] or for complexes like $[Me_2Si(C_5Me_4)(NPh)Yb(THF)_2]$[30] or the "ate" complex $[K(THF)_3]_2[Sm_2(C_{22}H_{28}N_4)_2](THF)_4$ ($C_{22}H_{28}N_4$ = TMTAT = tetramethyldibenzotetraaza[14]annulate)[10] The μ_2-bridging carbazolate ligands show a slight π-stacking towards the Sm^{II} center with relatively short Sm^{II}−C distances of 294(2) and 300(2) pm.

The Sm^{III} atoms are coordinated by five N atoms forming a distorted trigonal bipyramid. Two of the N atoms form μ_2 bridges to Sm^{II} centers, and two others belong to carbazolate ligands that coordinate in an η^6 fashion to another Sm^{II} center with one of their phenyl rings, thus forming the chain structure of **1**. The fifth nitrogen atom coordinated to Sm^{III} is not connected to any other samarium atom and is found in two disordered positions in the crystal structure. The Sm^{III}−N distances in $^1_\infty[Sm_2(Cbz)_5](CbzH)$ (**1**) range from 236(1) to 248.8(9) pm, the longer distances are located in the μ_2-bridges. Thus, **1** is similar to other trivalent Sm amides like $[(C_{11}H_{21}N_2)_2SmBr]$ ($C_{11}H_{21}N_2$ = 2-propylamino-4-propylimino-2-pentene) with Sm−N distances of 236−242 pm,[31] whilst homoleptic $[Sm(N\text{-MeIm})_8]I_3$ has longer Sm−N distances, averaging 260 pm, with the ligands having N-donor amine and not amide character.[31] The N−Sm^{III}−N angles in **1** are similar to those in an ideal trigonal bipyramid, with N1−Sm^{III}−N3 being 114.0(4)°, N2−Sm^{III}−N5 128.7(8)° and a stretched N2−Sm^{III}−N4 angle of 175.4(4)°. Figure 2 shows the dimeric building unit of **1** and the coordination spheres around Sm^{II} and Sm^{III}.

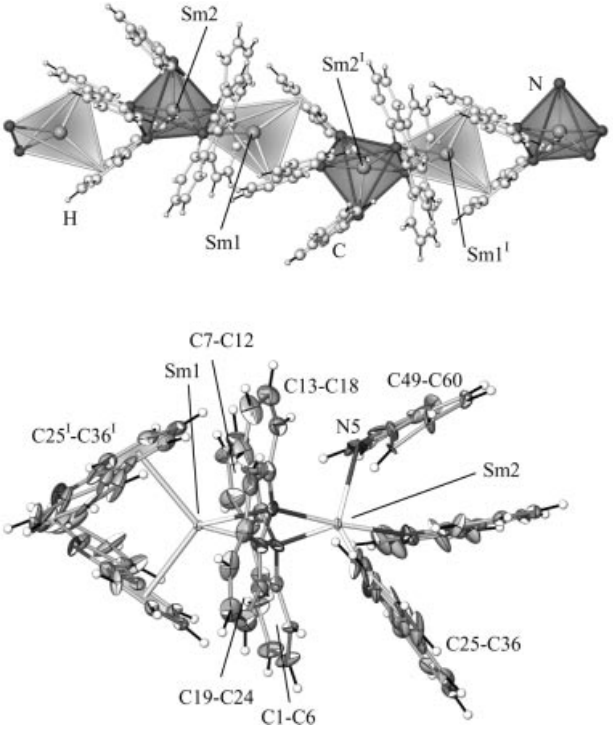

Figure 2. The coordination spheres around (top) and the dimeric building units of (bottom) divalent Sm1 and trivalent Sm2 in the chain structure of $^1_\infty[Sm_2(Cbz)_5](CbzH)$ (**1**); N−N connection lines mark only the coordination polyhedra and not bonds; π-interactions are marked by shaded planes and are represented by bonds towards centroids of the phenyl rings; the thermal ellipsoids here and in Figure 4 are scaled to a probability density of the atoms of 50%; symmetry operation: I: x, $-y + 3/2$, $z + 1/2$

The polymeric chains in the crystal structure of **1** leave tunnels between them, which are filled with carbazole molecules from the melt reaction. They are therefore not coordinated to the Sm centers and are released first in the thermal decomposition process. Figure 3 shows the crystal structure of $^1_\infty[Sm_2(Cbz)_5](CbzH)$ (**1**), including the chains

and tunnels. The crystal structure of **1** is unique in amide chemistry.

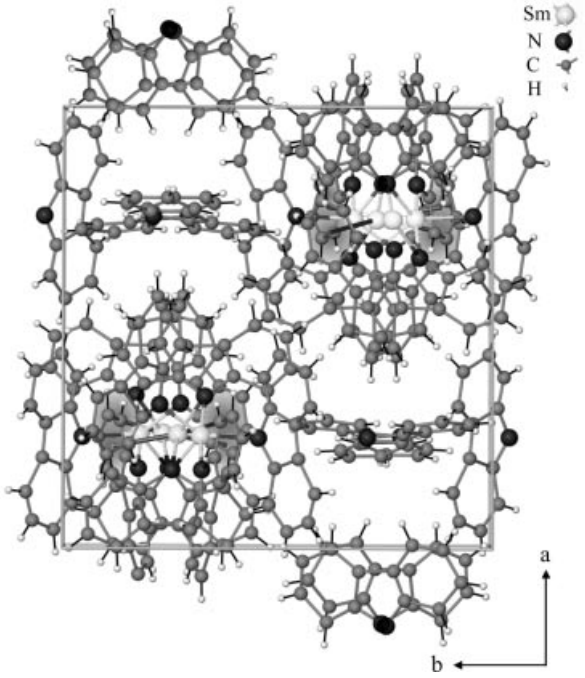

Figure 3. The crystal structure of $^{1}_{\infty}[Sm_2(Cbz)_5](CbzH)$ (**1**) with a view along the chain direction [00−1]; between the strands of $^{1}_{\infty}[Sm_2(Cbz)_5]$ run tunnels in which CbzH molecules are intercalated; η^6-interactions between Sm and phenyl rings are represented by bonds towards centroids and shaded rings

Despite the difference in stoichiometry, the dimeric building units of $[Tm_2(Cbz)_6]$ (**2**) resemble the divalent carbazolates $^{1}_{\infty}[Ln_2(Cbz)_4]$ (Ln = Eu, Yb).[18] Complex **2** also exhibits a tetrahedral coordination environment, with three nitrogen atoms and one η^6-coordinated phenyl ring. Contrary to the divalent carbazolates, however, the tetrahedra in the dimeric unit are not edge-connected by μ_2-bridging N atoms. With three carbazolate ligands coordinating each Tm atom, the linkage in the dimeric unit is formed by the N atoms of carbazolate ligands that use one of their phenyl rings to coordinate to the neighbouring Tm atom, similar to the coordination mode that forms the chains in $^{1}_{\infty}[Ln_2(Cbz)_4]$ (Ln = Eu, Yb)[18] as well as in **1**. As all the other carbazolate ligands in **2** do not connect further, Tm^{III} has a low coordination number of six and shows only dimers and no chains in the crystal structure. The dimeric units and coordination spheres around Tm^{III} in **2** are shown in Figure 4, while Figure 5 gives a view of the packing of the dimers in the crystal structure of **2**. The $Tm^{III}-N$ distances range from 220.8(3) to 228.2(3) pm, with the longest distance being found for the linking carbazolate ligands. These distances are in the region expected for the ionic radius of Tm^{III},[33] but shorter than in $[(Et_2C(C_4H_3N)_2]_3Tm][K(Tol)]_3$ (233−239 pm) or [(Et$_8$-calix[4]tetrapyrrole)Tm][K(DME)] [236−238 pm for the $Tm^{III}-N$(amide) bonds].[34] The Tm−centroid(3)distance to the π-coordinated phenyl rings in **2** is 244.2(4) pm, with Tm−π(C) bond lengths of 274.9(4)−288.7(3) ppm. The best comparable example to the η^6-phenyl−Tm interactions is found in $[Tm(DME)_2(\eta^2\text{-}C_{10}H_8)_2(\mu_2\text{-}\eta^4\text{:}\eta^4\text{-}C_{10}H_8)]$ with a Tm−π(C) distance of only 259−262 pm.[35] The coordination tetrahedron around Tm in **2** is more regular than in **1** [N1−Tm^{III}−N2: 108.1(1)°; N1−Tm−centroid(3): 122.8(1)°; N2−Tm−centroid(3): 112.2(1)°; see Table 1 for detailed atom distances and bond angles of **1** and **2**].

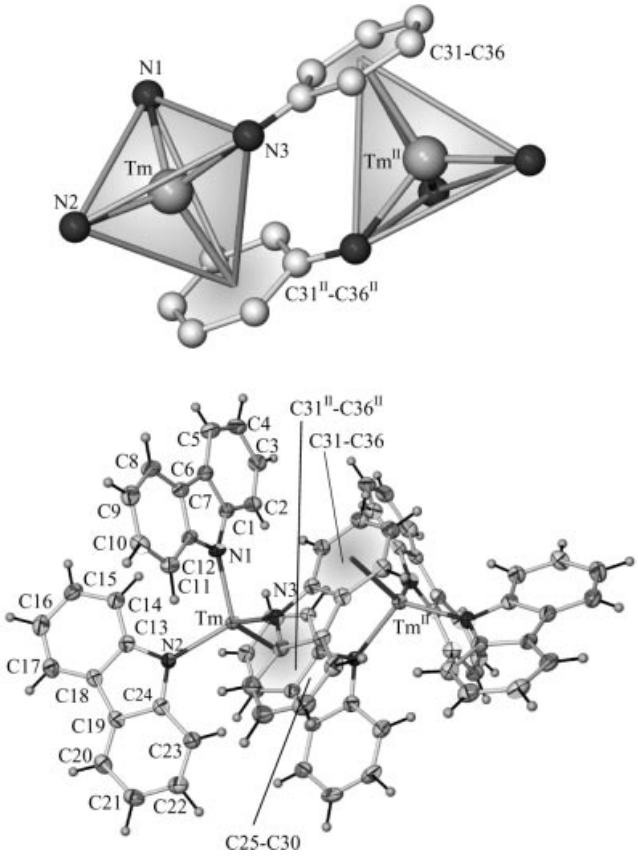

Figure 4. The coordination tetrahedra around Tm atoms (top) and the dimeric building units of $[Tm_2(Cbz)_6]$ (**2**, bottom); N−N connection lines mark only the coordination polyhedra and not bonds; π-interactions are marked by shaded planes and are represented by bonds towards centroids of the phenyl rings; symmetry operation: II: $-x, y, -z + 3/2$

The X-ray powder diffraction spectrum of $[Gd_2(Cbz)_6]$ (**4**) shows that the compound is isotypic to $[Tm_2(Cbz)_6]$ (**2**). Thus, the description of the crystal structure in the space group *Pbcn* is analogous to that of **2**. Because of the larger ionic radius of Gd^{III} compared to Tm^{III},[33] the unit cell is about 300×10^6 pm^3 larger than in **2**. $[Nd_2(Cbz)_6]$ (**3**) is not isotypic to **2**. The powder diffractogram of **3** can be indexed to give an orthorhombic cell of about half the size of the unit cell of **2**, with no unindexed lines. The large difference in the ionic radii of Nd^{III} and Tm^{III} is responsible for a different unit cell and thereby a different crystal structure. Considering this difference a tripled unit cell of **3** shows a volume increase of about 300×10^6 pm^3 compared to Gd^{III} in **4** or 600×10^6 pm^3 compared to Tm^{III} in **2**, and therefore is in good accordance with the radii increase throughout the series of rare-earth elements. Though the

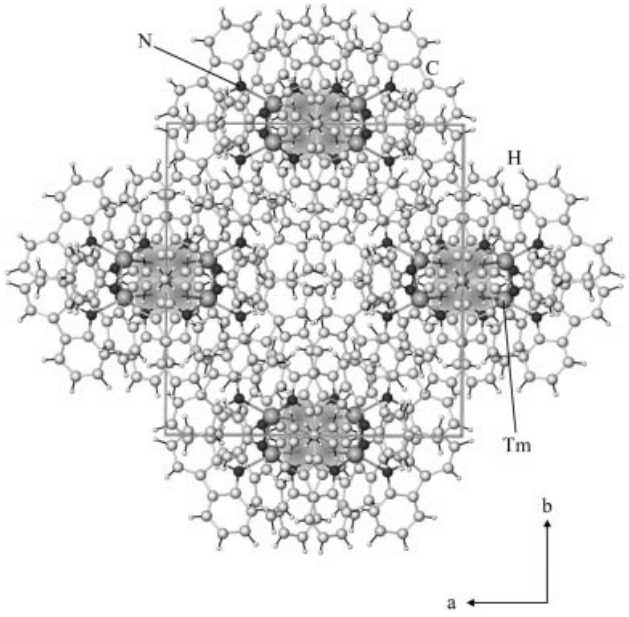

Figure 5. The crystal structure of $[Tm_2(Cbz)_6]$ (**2**) with a view of the unit cell along [001]; without further interaction between the dimeric units, the structure is a packing of dimers; η^6-interactions between Tm and phenyl rings are represented by bonds towards centroids and shaded rings

structure of **2** and **4** makes it likely that **3** also forms dimeric units, this remains unproven. Together with the results of microanalyses and the MIR and FIR spectra, the powder diffraction investigations of **3** and **4** confirm the trivalent character of neodymium and gadolinium as well as the absence of uncoordinated carbazole molecules in the structures.

Conclusions

The formation of **1**−**4** shows the possibility of obtaining homoleptic amides of the rare-earth elements that is an inherent feature of solvent-free melt synthesis methods. In the absence of any coordinating solvent the carbazolate ligands have no option but to completely saturate the coordination sphere around the large rare-earth ions. The results are structures that are unique in rare-earth amide chemistry and depend on additional η^6-π interactions as well as normal σ-N bonds. The course of the redox potentials from $E_{Eu^{II/III}} = 0.35$ V to $E_{Sm^{II/III}} = 1.57$ V and $E_{Tm^{II/III}} = 2.27$ V, $E_{Nd^{II/III}} = 2.62$ V up to $E_{Gd^{II/III}} = 3.9$ V[21,22] reflects the valences of the homoleptic carbazolates. Whilst divalent Eu and Yb compounds can be obtained,[18] Sm is mixed-valent in **1** with alternating Sm^{II} and Sm^{III}. Tm already gives pure trivalent **2**. Accordingly, all other rare-earth elements with redox potentials higher than Tm can also be expected to give trivalent compounds, as is shown by the neodymium and gadolinium carbazolates **3** and **4**. Due to the different stoichiometries, divalent, mixed-valent and trivalent homoleptic carbazolates, although having some common structural elements, have completely different crystal structures. Additional analytic methods like IR and Raman spectroscopy or thermal analysis support the results of the X-ray crystal-structure determinations.

Experimental Section

General: All reactions were carried out under argon using standard dry-box and Schlenk techniques due to the air and moisture sensitivity of **1**−**4**. Samarium, thulium, gadolinium (ChemPur), neodymium (STREM) and carbazole (Aldrich) were used as purchased. The IR spectra were recorded using a Bruker FTIR-IS66V-S spectrometer, and the Raman spectra using a Bruker FRA 106-S spectrometer. Probably because of its dark colour, **1** gave no Raman spectrum. KBr pellets were used for MIR investigations and PE pellets for FIR investigations, both under vacuum. The thermal decomposition of **1** was studied using simultaneous DTA/TG (NETZSCH STA-409). A 16.9 mg sample of the bulk of the Sm reaction was heated from 20 °C to 700 °C at a heating rate of 10 °C/min in a constant Ar flow of 60 mL/min. The thermal decomposition of **2** was studied on 17.0 mg of the bulk of the Tm reaction from 20 °C to 700 °C at a heating rate of 10 °C/min in a constant Ar flow of 60 mL/min. The thermal decomposition of **3** was studied on 38.8 mg of the bulk of the Nd reaction, and the thermal decomposition of **4** was studied on 24.3 mg of the bulk of the Gd reaction under analogous conditions to the investigations for **1** and **2**.

$^1_\infty[Sm_2(Cbz)_5](CbzH)$ (1): Samarium metal (150 mg, 1×10^{-3} mol) and carbazole (CbzH, $C_{12}H_8NH$; 501 mg, 3×10^{-3} mol) were sealed in an evacuated Duran glass ampoule. The reaction mixture was heated to 220 °C over 4 h and then to 265 °C in another 7 h. This temperature was maintained for 190 h. The melt was cooled to 200 °C over 70 h and then to room temperature over 24 h. Except for the excess of Sm metal and CbzH the reaction was complete giving a mixture of dark red to black microcrystals and black to dark red rod-shaped crystals of $^1_\infty[Sm_2(Cbz)_5](CbzH)$ with a length of 0.3 to 0.8 mm. Yield: 580 mg (89%). MIR: $\tilde{\nu}$ = 3418 s, 3049 m, 1615 m, 1603 m, 1585 m, 1580 msh, 1493 m, 1482 m, 1459 s, 1450s, 1433 s, 1336 s, 1326 m, 1288 m, 1273 s, 1262 ssh, 1236 m, 1146 m, 1118 m, 1106 m, 997 m, 927 m, 884 m, 844 m, 750 vs, 725 vs, 664 w, 569 w cm^{-1}. FIR: $\tilde{\nu}$ = 522 w, 508 w, 430 m, 424 m, 305 w, 231 m, 171 m, 146 w, 123 w, 108 w cm^{-1}. $C_{72}H_{49}N_6Sm_2$ (1298.9): calcd. C 66.63, H 3.78, N 6.48; found C 66.22, H 3.75, N 6.62.

$[Tm_2(Cbz)_6]$ (2): Thulium metal (85 mg, 5×10^{-4} mol), carbazole (334 mg, 2×10^{-3} mol) and Hg (0.2 g) were sealed in an evacuated Duran glass ampoule. The reaction mixture was heated to 240 °C over 4 h and then to 280 °C over another 3 h. This temperature was maintanied for 168 h. The melt was then cooled to 210 °C over 200 h and then to room temperature over 72 h. Except for a slight excess of Tm metal and CbzH, the reaction was complete, giving an orange crystalline bulk of crystals of $[Tm_2(Cbz)_6]$ with a length of 0.2 to 0.5 mm. Yield: 313 mg (94%). MIR: $\tilde{\nu}$ = 3419 w, 3049 m, 1618 w, 1602 m, 1493 m, 1458 ssh, 1450 vs, 1430 m, 1327 s, 1288 w, 1271 w, 1239 s, 1207 m, 1148 w, 1108 w, 1025 w, 1015 w, 932 m, 905 m, 848 w, 749 vs, 726 vs, 574 m cm^{-1}. FIR: $\tilde{\nu}$ = 432 m, 420 m, 343 w, 309 w, 251 m, 188 vw, 158 w, 143 w, 86 w cm^{-1}. Raman: $\tilde{\nu}$ = 3054 s, 1620 s, 1588 w, 1570 s, 1565 ssh, 1480 m, 1316 m, 1271 m, 1248 m, 1015 m, 744 m, 680 m, 310 w, 251 s, 200 w, 170 w, 157 w, 91 vs cm^{-1}. $C_{72}H_{48}N_6Tm_2$ (1335.1): calcd. C 64.77, H 3.62, N 6.29; found C 63.93, H 3.77, N 6.07.

$[Nd_2(Cbz)_6]$ (3): Neodymium metal (144 mg, 1×10^{-3} mol), carbazole (1032 mg, 6×10^{-3} mol) and Hg (0.2 g) were sealed in an

evacuated Duran glass ampoule. The reaction mixture was heated to 230 °C over 8 h and then to 280 °C over another 5 h. The melt was cooled to 245 °C over 350 h and this temperature maintained for 168 h. The reaction mixture was then cooled to 210 °C over another 350 h and to room temperature over 72 h. Except for the excess CbzH, the reaction gave a golden yellow bulk of $[Nd_2(Cbz)_6]$. Yield: 548 mg (85%). MIR: $\tilde{\nu}$ = 3419 w, 3049 m, 1625 w, 1601 m, 1493 m, 1456 ssh, 1450 vs, 1426 w, 1394 w, 1336 m, 1327 s, 1286 w, 1238 s, 1205 w, 1138 w, 1106 w, 1009 w, 996 w, 928 m, 914 w, 857 w, 842 w, 748 vs, 725 vs, 574 s, 564 ssh cm^{-1}. FIR: $\tilde{\nu}$ = 440 m, 425 m, 352 w, 221 m, 145 m, 123 m, 102 w, 70 w cm^{-1}. Raman: $\tilde{\nu}$ = 3056 s, 1625 s, 1573 s, 1480 w, 1311 s, 1311 s, 1289 s, 1260 w, 1011 s, 741 m, 430 m, 280 m, 230 m, 104 s cm^{-1}. $C_{72}H_{48}N_6Nd_2$ (1291.1): calcd. C 66.98, H 3.72, N 6.51; found C 66.37, H 3.96, N 6.47.

$[Gd_2(Cbz)_6]$ (4): Gadolinium metal (157 mg, 1×10^{-3} mol), carbazole (668 mg, 4×10^{-3} mol) and Hg (0.2 g) were sealed in an evacuated Duran glass ampoule. The reaction mixture was heated to 200 °C over 6 h and to 280 °C over another 8 h for activation. The melt was cooled to 245 °C over 4 h and the temperature maintained for 336 h. The reaction mixture was then cooled to 210 °C over another 180 h and then to room temperature over 24 h. Except for the excess of CbzH the reaction gave a poorly crystalline dark yellow bulk of $[Gd_2(Cbz)_6]$. Yield: 526 mg (80%). MIR: $\tilde{\nu}$ = 3417 w, 3050 m, 1603 s, 1581 m, 1492 s, 1471 ssh, 1450 vs, 1426 m, 1407 s, 1325 vs, 1263 w, 1237 vs, 1207 msh, 1149 w, 1118 w, 1025 w, 1015 w, 930 w, 906 w, 750 vs, 726 vs, 569 m cm^{-1}. FIR: $\tilde{\nu}$ = 444 w, 430 m, 420 m, 363 w, 243 m, 231 wsh, 159 m, 148 wsh, 72 w cm^{-1}. Raman: $\tilde{\nu}$ = 3055 s, 1624 s, 1570 s, 1481 m, 1311 s, 1288 m, 1261 m, 1011 s, 742 m, 429 m, 297 m, 258 m, 240 w, 101 s cm^{-1}. $C_{72}H_{48}N_6Gd_2$ (1317.1): calcd. C 65.65, H 3.64, N 6.38; found C 65.74, H 3.70, N 6.39.

X-ray Crystal-Structure Determination: The data collection for single-crystal X-ray determinations of **1** and **2** were carried out with an IPDS-II diffractometer (STOE). Structure solutions: SHELXS-86;[36] structure refinements: SHELXL-97.[37] Integrity of symmetry and geometry: PLATON.[38] All non-hydrogen atoms were refined anisotropically. The hydrogen atoms of **2** were found in the Fourier map while the hydrogen atoms of **1** were placed in calculated positions and assigned to an isotropic displacement parameter of 1.2-times the size of the isotropic displacement parameter of the parent carbon atom. The nonlinking Cbz anion of **1** is disordered over two positions in a ratio of about 1:1. The crystal of **1** used for data collection shows another small crystalline individual grown on the surface (RECIPE).[39] The two individuals were separated (TWIN)[39] and refined individually. Compounds **3** and **4** were investigated on powder samples in sealed capillaries with a STOE STADI P transmission diffractometer (Cu-$K_{\alpha 1}$ radiation λ = 1.540598 Å, focussed single crystal germanium monochromator). Because **3** and **4** lose their crystallinity upon grinding, samples of both compounds had to be made only roughly homogeneous. Both were investigated in 0.5 mm capillaries, though this led to a higher background due to absorption phenomena of the rare-earth atoms. The diffraction patterns of the neodymium (**3**) and the gadolinium (**4**) compounds were compared with simulated diffractograms of **1** and **2** as well as the divalent europium and ytterbium carbazolates.[18] The cell constants of **3** were refined on 11 reflections with the best possible resolution leading to an orthorhombic unit cell without un-indexed lines and an average $\delta(2\Theta)$ of 0.018° [T = 293(2) K, a = 1899(2) pm, b = 1118.5(9), c = 920(1) pm, V = 1953.5(26) 10^6 pm^3]. The cell constants of **4** were refined on 23 reflections with the best possible resolution without un-indexed lines and an average $\delta(2\Theta)$ of 0.016° [T = 293(2) K, a = 1723(1) pm, b = 1888(1), c = 1710.5(9) pm, V = 5569.7(32) 10^6 pm^3], indicating that $[Gd_2(Cbz)_6]$ is isotypic with $[Tm_2(Cbz)_6]$ (**2**).[40] Crystallographic data for $C_{72}H_{49}N_6Sm_2$ (**1**): Monoclinic, $P2_1/c$, Z = 4, T = 170(1) K, a = 1835.3(2), b = 1657.0(2), c = 1937.9(2) pm, β = 112.138(8)°, V = 5458.8(1)·10^6 pm^3, μ = 21.8 cm^{-1} (Mo-K_α), 3.34° ≤ 2θ ≤ 50.0°, −21 ≤ h ≤ 20, −19 ≤ k ≤ 19, 0 ≤ l ≤ 23, F(000) = 2584, R_1 = 0.0745 for 4644 reflections [$I > 2\sigma(I)$], R_1 = 0.1288 and wR_2 = 0.1208 for all 9545 unique reflections, GOOF on F^2 = 0.886. Crystallographic Data for $C_{72}H_{48}N_6Tm_2$ (**2**): Orthorhombic, $Pbcn$, Z = 4, T = 170(1) K, a = 1712.2(2) pm, b = 1802.5(2) pm, c = 1699.7(2) pm, V = 5245.9(9)·10^6 pm^3, μ = 34.1 cm^{-1} (Mo-K_α), 3.28° ≤ 2θ ≤ 54.64°, −21 ≤ h ≤ 21, −23 ≤ k ≤ 23, −18 ≤ l ≤ 21, F(000) = 2640, R_1 = 0.0249 for 4147 reflections [$I > 2\sigma(I)$], R_1 = 0.0430 and wR_2 = 0.0581 for all 5831 unique reflections, GOOF on F^2 = 0.926. CCDC-220967 (**1**) and -241797 (**2**) contain the supplementary crystallographic data for this paper. These data can be obtained free of charge at www.ccdc.cam.ac.uk/conts/retrieving.html [or from the Cambridge Crystallographic Data Centre, 12 Union Road, Cambridge CB2 1EZ, UK; Fax: + 44 1223-336-033; E-mail: deposit@ccdc.cam.ac.uk].

Acknowledgments

We are grateful to the Fonds der Chemischen Industrie and Prof. Dr. Gerd Meyer for financial support.

[1] G. Wilkinson, J. M. Birmingham, *J. Am. Chem. Soc.* **1954**, *76*, 6210.
[2] R. G. Hayes, J. L. Thomas, *J. Am. Chem. Soc.* **1969**, *91*, 6876.
[3] H. Schumann, *Angew. Chem.* **1984**, *96*, 475−493; *Angew. Chem. Int. Ed. Engl.* **1984**, *23*, 474−492.
[4] R. Kempe, *Angew. Chem.* **2000**, *112*, 478−504; *Angew. Chem. Int. Ed.* **2000**, *39*, 468−494.
[5] H. Schumann, J. A. Meese-Marktscheffel, L. Esser, *Chem. Rev.* **1995**, *95*, 865−986.
[6] S. Arndt, J. Okuda, *Chem. Rev.* **2002**, *102*, 1953−1976.
[7] W. J. Evans, B. L. Davis, *Chem. Rev.* **2002**, *102*, 2119−2136.
[8] Cambridge Crystallographic Data Centre, CCDC, 12 Union Road, Cambridge CB2 1EZ, Great Britain.
[9] A. de Cian, M. Moussavi, J. Fischer, R. Weiss, *Inorg. Chem.* **1985**, *24*, 3162.
[10] J. Magull, A. Simon, *Z. Anorg. Allg. Chem.* **1992**, *618*, 81−86.
[11] R. Kempe, H. Noss, T. Irrgang, *J. Organomet. Chem.* **2002**, *647*, 12−20.
[12] G. B. Deacon, A. Gitlits, B. W. Skelton, A. H. White, *Chem. Commun.* **1999**, 1213−1214.
[13] G. B. Deacon, A. Gitlits, P. W. Roesky, M. R. Bürgstein, K. C. Lim, B. W. Skelton, A. H. White, *Chem. Eur. J.* **2001**, *7*, 127−138.
[14] K. Müller-Buschbaum, *Z. Anorg. Allg. Chem.* **2002**, *628*, 2731−2737.
[15] K. Müller-Buschbaum, C. C. Quitmann, *Inorg. Chem.* **2003**, *42*, 2742−2750.
[16] K. Müller-Buschbaum, *Z. Anorg. Allg. Chem.* **2003**, *629*, 2127−3132.
[17] K. Müller-Buschbaum, C. C. Quitmann, *Z. Anorg. Allg. Chem.* **2004**, *630*, 131−136.
[18] K. Müller-Buschbaum, C. C. Quitmann, *Z. Anorg. Allg. Chem.* **2003**, *629*, 1610−1616.
[19] W. J. Evans, G. W. Rabe, J. W. Ziller, *Organometallics* **1994**, *13*, 1641−1645.
[20] G. B. Deacon, C. M. Forsyth, B. M. Gatehouse, P. A. White, *Aust. J. Chem.* **1990**, *43*, 795−806.
[21] L. R. Morss, *Chem. Rev.* **1976**, *76*, 827−841.
[22] G. Meyer, *Chem. Rev.* **1988**, *88*, 93−107.
[23] W. F. Hemminger, H. K. Cammenga, *Methoden der Thermischen Analyse*, Springer Verlag, **1989**.

[24] G. Ostendorp, H. W. Rotter, H. Homborg, *Z. Anorg. Allg. Chem.* **1996**, *622*, 235−244.
[25] B. Schrader, *Raman/Infrared Atlas of Organic Compounds*, 2nd ed., Wiley-VCH, Weinheim, **1989**.
[26] J. Weidlein, U. Müller, K. Dehnicke, *Schwingungsfrequenzen II, Nebengruppenelemente*, Georg Thieme Verlag, Stuttgart, **1986**.
[27] P. C. Davidson, M. F. Lappert, R. Pearce, *Acc. Chem. Res.* **1974**, *7*, 209−217.
[28] C. C. Quitmann, K. Müller-Buschbaum, *Z. Anorg. Allg. Chem.* **2004**, *630*, in press.
[29] T. Dube, M. Ganesan, S. Conoci, S. Gambarotta, G. P. A. Yap, *Organometallics* **2000**, *19*, 3716−3721.
[30] Z. Hou, T. Koizumi, M. Nishiura, Y. Wakatsuki, *Organometallics* **2001**, *20*, 3323−3328.
[31] W. J. Evans, G. W. Rabe, J. W. Ziller, *Inorg. Chem.* **1994**, *33*, 3072−3078.
[32] D. Drees, J. Magull, *Z. Anorg. Allg. Chem.* **1995**, *621*, 948−952.
[33] R. D. Shannon, *Acta Crystallogr., Sect. A* **1976**, *32*, 751−767.
[34] I. Korobkov, G. Aharonian, S. Gambarotta, G. P. A. Yap, *Organometallics* **2002**, *21*, 4899−4901.
[35] M. N. Bochkarev, I. L. Fedushkin, A. A. Fagin, H. Schumann, J. Demtschuk, *Chem. Commun.* **1997**, 1783−1784.
[36] G. M. Sheldrick, *SHELXS-86, Program for the resolution of crystal structures*, Göttingen, **1986**.
[37] G. M. Sheldrick, *SHELXL-97, Program for the refinement of crystal structures*, Göttingen, **1997**.
[38] A. L. Spek, *PLATON-99, A Multipurpose Crystallographic Tool*, Utrecht, **1999**.
[39] *STOE Software Package*, version 1.16, *RECIPE, Program for the identification of crystalline individuals* and *TWIN, Program for the separation of crystalline individuals*, Wiesbaden, **2001**.
[40] *STOE WINXPOW, Program package for the operation of powder diffractometers and analysis of powder diffractograms*, version 1.04, Darmstadt, **1999**.

Received June 15, 2004
Early View Article
Published Online August 26, 2004

